Peer Reviewed
2017 Solar Research Conference

ASIA-PACIFIC
SOLAR RESEARCH
CONFERENCE

**D K Bisset**

# Images Formed by a Piecewise-Focusing Solar Collector

David K Bisset

*Canberra ACT*

*E-mail: davidkbisset@gmail.com*

**Abstract**

The concept of the piecewise-focusing (PWF) solar collector for use in concentrating solar thermal (CST) power stations, realised as a 'segmented dish', is analyzed experimentally and numerically. A scale model of one mirror unit gave corner-ray intersections on the target plane that agreed quite well with the numerical model over a wide range of sun elevations. Applied to a representative group of mirror units, the numerical model shows that focus quality at a concentration ratio of 2000 (required for a cavity receiver) is satisfactory at all except very low sun elevations. For adequate focusing at all elevations the number of mirror units per PWF collector must be increased from 80 to 200-300. Compared to a large central receiver CST plant with a surround-field of heliostats, a PWF and cavity receiver CST plant requires only 70% of the mirror area for the same heat rate.

## 1. Introduction

This paper continues the work on piecewise-focusing (PWF) solar collectors for use in concentrating solar thermal power generation begun by Bisset (2016). Figure 1 (repeated from that paper) shows the concept of the PWF collector, in which the scales of vertical and horizontal sun-tracking motion are separated. Around 100 individual mirror units, mounted on a base-frame, track the sun's elevation, and the entire base-frame tracks the sun in azimuth. Each mirror unit rotates about a single nearly-horizontal axis attached at a particular angle to the base frame; single-axis sun elevation tracking is a key aspect for cost reduction. Although the overall shape of the collector is arbitrary, the

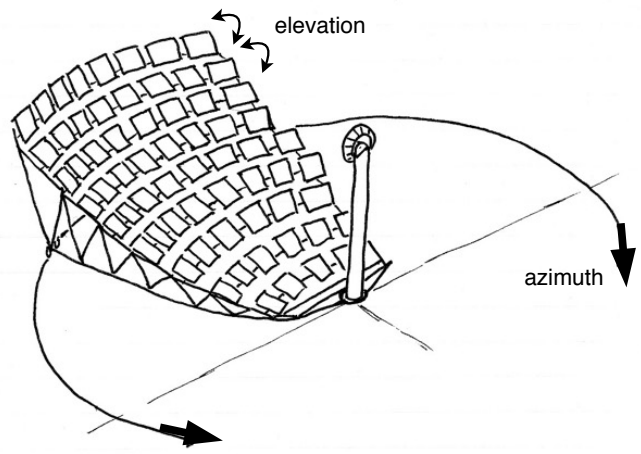


**Figure 1. Concept sketch**

concept is realised here as a 'segmented dish', in which the mirror units approximate the surface of a paraboloid tilted at a fixed angle (Figure 2).

An advantage of large-scale azimuthal tracking is that a collector's reflecting surfaces are always nearly square-on to the sun, minimizing cosine losses and astigmatism. For example, azimuthal rotation (or equivalent) is integral to the tracking motion of the paraboloidal dish, the most efficient optically of all solar concentrators. In contrast, the heliostats of a central receiver system are fixed to the earth and their mirrors are quite oblique to the sun for large parts of the day. However, the size of a dish is severely limited by the need to raise the entire collector for sun elevation tracking, and therefore several designs have been proposed for 'moving fields' of multiple reflectors that are rotated azimuthally as a group. Baum et al (1957) designed a system of tilting mirrors mounted on trains of carriages travelling on 23 concentric tracks around a central tower-mounted boiler, and built a 1:50 scale model. Jones (1982; also see Kolb et al, 2007) proposed numerous 2-axis tilting mirrors on a large azimuthally-rotating platform. Ruiz et al (2014) designed, and have partly constructed, a series of concentric tracks and trolleys for moving a field of conventional heliostats azimuthally around a tower-mounted receiver.

The gain in efficiency compared to a well-designed polar (static) field of heliostats is around 8-10% (Ruiz et al, 2014), and it is debatable whether this is sufficient to outweigh the extra complications of tracks and trolleys. The Baum et al (1957) design offset those complications by using much simpler single-axis tilting mirrors, with each axis inclined at a specific angle to its carriage depending on its position within the field. The method for deriving these inclinations was not known to the present author until recently, and although presented differently it appears to be equivalent to the method for finding axis angles in PWF collector

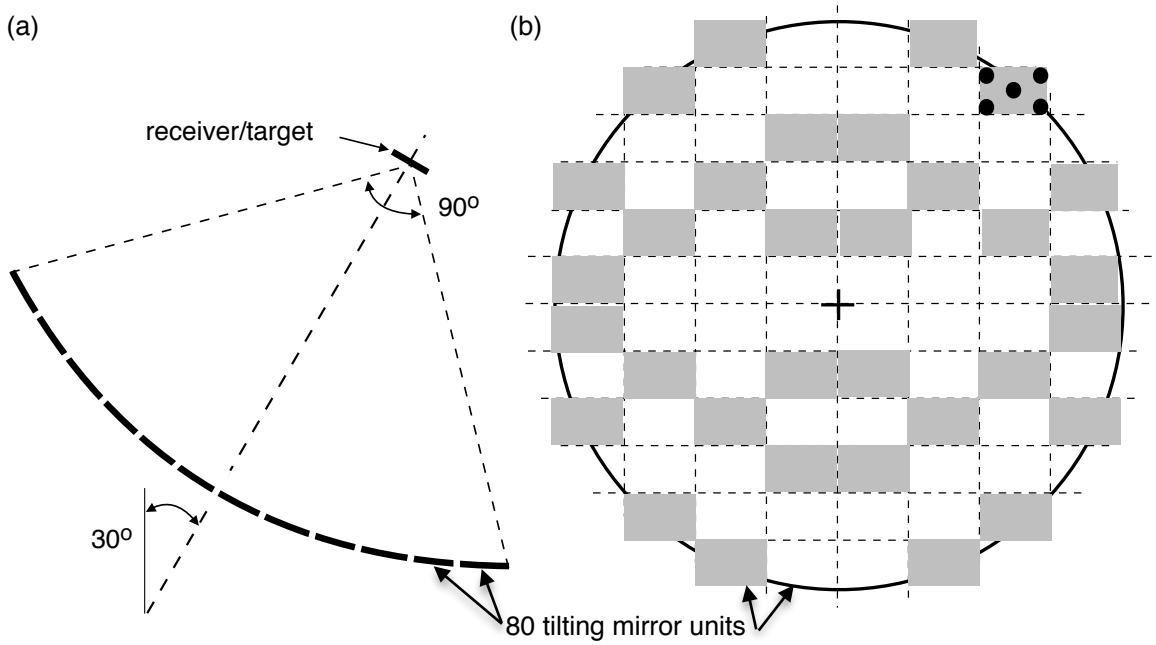


**Figure 2. The segmented dish. (a) Side view cross-section. (b) View into the aperture. Grey: mirror units for the numerical model. Dots: unit for the physical scale model.**

design (Bisset, 2016). It was stated (Baum et al, 1957) that deviations of mirror-normals from true directions did not exceed 1' 15'' (0.36 milliradians); details were not given, but the result is comparable to the deviations found by Bisset (2016) for the PWF segmented dish.

The general aims for improving collector fields in concentrating solar thermal (CST) power plants are to maximize the heat collected per $m^2$ of reflector, and to minimize the overall cost per $m^2$. The tiered base-frame of the PWF concept is strong, light, inexpensive, and brings the mirror units close together without much shading or blocking — collection efficiency is close to that of a standard paraboloidal dish. Single-axis mounting of mirror units on the base-frame reduces cost compared to dual-axis heliostats, and the receiver can be a high-efficiency cavity receiver as for standard dishes. However, the feasible size of one PWF collector (though an order of magnitude larger than for standard dishes) is too small for CST power plants, and therefore multiple collectors are required. For this reason it is desirable to keep the number of mirror units per collector as small as possible by using relatively large mirror units, which may suffer from astigmatism. Also it is not certain that molten salt from a thermal storage would be satisfactory as the heat transfer fluid in the PWF receivers (the practice in recent central receiver CST plants). These points are analyzed and/or discussed in the following.

## 2. Aiming errors from the corners of mirror units

Single-axis mounting of each mirror unit is crucial for cost reduction, but it means that mirror unit aim as the sun elevation varies cannot be perfect in general. However, Bisset (2016) showed that aiming errors (as a function of sun elevation) from the centres of mirror units are quite small. The relatively large size of mirror units is potentially a more serious problem, and aims from the corners of a unit deviate much more than aim from its centre, causing astigmatism at low and high sun elevations. The PWF segmented dish used for this work

**Figure 3. The 5/3-scale model (right), tilted towards the sun for higher apparent sun elevation, and the mirror unit (left). White circles indicate mirror mounting points.**

(Figure 2) has only 80 mirror units covering its aperture, whereas the moving field designs mentioned above contain much larger numbers of relatively smaller reflectors: 624 (Ruiz et al, 2014), 1293 (Baum et al, 1957), or 2200 (Jones, 1982).

A numerical model to find intersections between reflected rays from non-central points and the target was developed previously and compared qualitatively with a physical collector model (Bisset, 2016). A more thorough test of the numerical model was warranted before further use of it in the present work. For this purpose a physical model of one mirror unit (indicated in Figure 2b) and the target was built, scaled by a factor of 5/3 relative to the previous model (aperture radius 3.0 m vs 1.8 m). The new model and a closer view of the 750 x 500 mm mirror unit are shown in Figure 3. The mirror unit chosen is at the edge of the aperture in one of the areas where axis inclinations are largest — i.e. it is a 'worst case' position. The closeup view gives an idea of how the mirror unit axis is turned counterclockwise (in this case) in the horizontal plane, and of how the mirror tangent plane is set at a considerable angle (25.3$^{o}$ in this case) to its mounting axis (white dashed line). The axis was determined using sun elevations of (15$^{o}$,45$^{o}$,75$^{o}$). Since data were wanted for sun elevations up to 80$^{o}$, but the maximum elevation on the days of the experiments was less than 60$^{o}$, the model was tilted towards the sun to obtain readings at higher apparent elevations, as

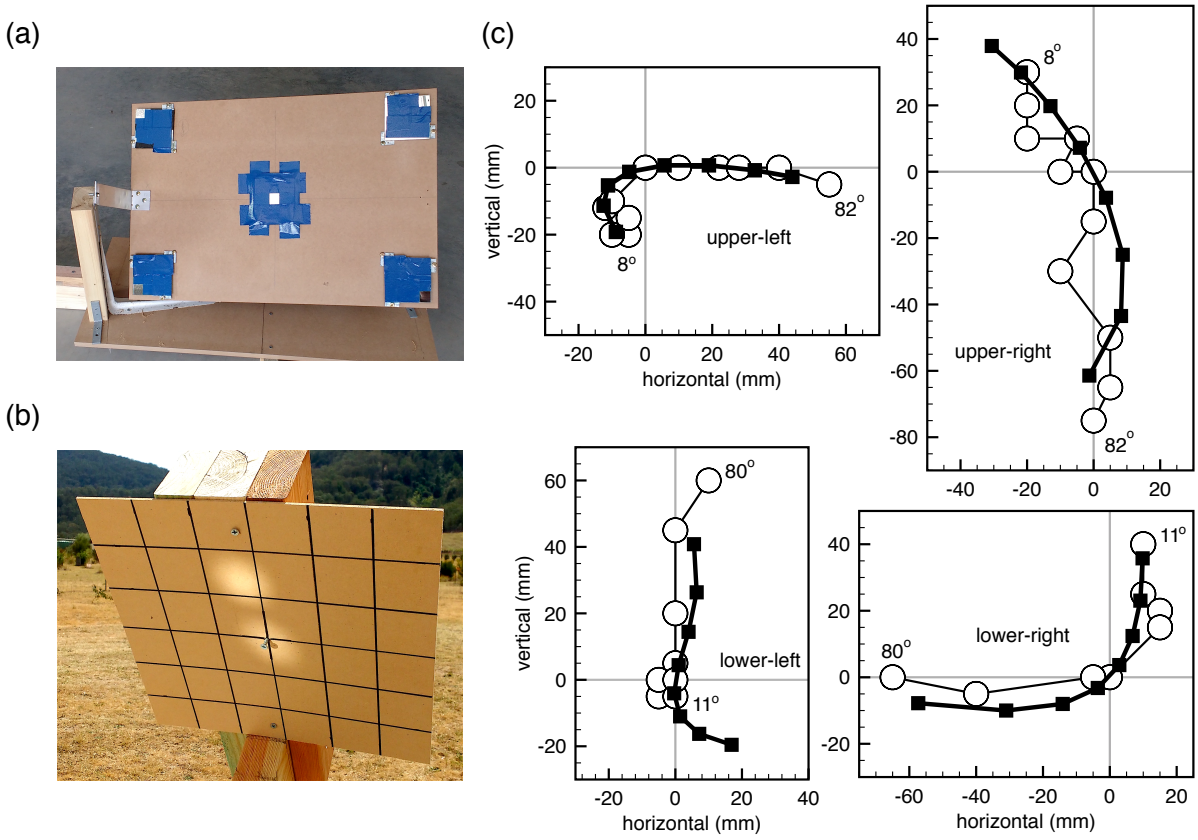


**Figure 4. Model results. (a) Mirror tiles masked at 25 x 25 mm. (b) An image on the target from the centre and one corner. (c) Physical (circles) and numerical (squares) intersection positions from corner rays as a function of sun elevation.**

pictured in Figure 3. The mirror unit was equipped with 100 x 100 mm mirror tiles at its centre and corners, masked down to 25 x 25 mm (Figure 4(a)). Corner aims were set with the sun at 45$^{o}$ elevation. An example of an image on the target (which has a 50 mm square grid) is given in Figure 4(b). It can be seen that the image spreads considerably because of the finite size of the sun, and therefore it is difficult to assess the position of the centre of each patch of light with precision better than about ±10 mm.

Numerical and physical results for corner ray intersections with the target are compared in Figure 4(c). Numerical results are given from sun elevations 10$^{o}$ to 80$^{o}$ at 10$^{o}$ intervals; physical results are given at various elevations between the endpoints shown. An unquantifiable amount of slack was present in the mirror tile aim adjustment screws, which combined with the imprecision in picking the centre of each patch of light on the target to add a bit of randomness to the results. Nevertheless, the overall agreement between physical and numerical results is sufficient to give confidence in the numerical modelling that follows.

## 3. Parameters for a cavity receiver

A true cavity receiver has a small opening through which concentrated sunlight passes and a much larger internal area of absorber surface. If the exterior is well insulated, heat is lost only from the entrance, by blackbody radiation and by mixed convection (passive and wind-driven). Kim, Kim and Stein (2015) computed heat losses from several types of receiver, including an external receiver equivalent to the cylindrical panels of a typical central receiver CSP plant, and a cavity receiver with an entrance area 1/20 of the absorber area. For example, at 600$^{o}$ C[1] and 5 m/s wind speed the heat loss rate (averaged over head-on and side-on wind directions) was 41.6 kW/m$^2$ for the external receiver but only 3.3 kW/m$^2$ of absorber for the cavity. From data in Pacheco (2002, Solar Two) and Sanchez-Gonzalez et al (2016, Gemasolar) it can be inferred that the average solar flux incident on molten-salt-type central receivers at solar noon is of order 400 kW/m$^2$ (and rather less when averaged over the course of a day), so a cavity receiver can improve collection efficiency by about 9% compared to external receivers. The cavity receiver also avoids the problem of surface reflectivity, where imperfect absorption results in the reflection of (typically) 5-7% of the flux incident on the absorber (Pacheco, 2002; Ho, 2017).

Assuming typical solar DNI and mirror reflectivity values, 400 kW/m$^2$ requires a geometrical concentration ratio (CR) of about 450, and therefore the CR required at the entrance to the cavity receiver modelled by Kim, Kim and Stein (2015) would be 9000 (20 times higher) — probably not realistic for a PWF collector. However, the entrance area of the cavity receiver designed by Pye et al (2015) is about 1/10 of the internal wall area (estimated from their Figure 3), and it achieves over 97% efficiency generating steam at 500$^{o}$ C (Coventry and Andraka, 2017). Also, absorber flux is pushed to the limit in central receivers to minimize size and therefore heat loss, whereas a larger absorber area in cavity receivers has little effect on heat loss, and the lower flux allows for possible use of compressed gas as the heat transfer

[1] This is the surface temperature, which can be much higher than the temperature of the heat transfer fluid — Kim, Kim and Stein (2015) used a difference of 100 K.

fluid. If the CR at the absorber surface is reduced to 200, and the entrance area is 1/10 of the absorber area, the required CR at the cavity entrance is 2000. For comparison, 2000 is also the ratio required for >95% reflected sunlight capture at the entrance to the receiver of the ANU SG4 paraboloidal dish (Lovegrove, Burgess and Pye, 2011).

## 4. Images formed on the target plane

The 32 mirror units indicated in Figure 2(b) were added to the numerical model, and intersection points on the target plane were calculated for the centres and corners of all units. As for the single unit above, the collector aperture radius was 3000 mm, mirror axes were determined using sun elevations of (15$^o$,45$^o$,75$^o$) and the corner aims were set with the sun at 45$^o$. In Figure 5 the intersection points are combined into images (focus maps) on a target plane that represents the entrance to a cavity receiver, at a range of sun elevations. Each intersection of a reflected ray with the target is indicated by a dot, but in practice the finite size of the sun would blur that dot by 15-20 mm in all directions. The larger circle indicates a CR of 2000, and the smaller dashed circle allows for blurring caused by the finite size of the sun. Local slope errors on the mirror surfaces are not accounted for, but on the other hand the points on the figures come from the extreme corners of the mirror units and reflected light from the remainder of each unit is better aimed. Note that although the apparent changes in CR at the cavity entrance are quite large, the light rays arrive in a cone shape with a 90$^o$ vertex angle and fan out similarly inside the cavity. The vertex of the cone becomes sharper at intermediate sun elevations but the effect on the cavity interior walls is quite small.

Figure 5 shows that collector focus is very satisfactory for sun elevations between about 30$^o$ and 70$^o$, but focus at 20$^o$ is borderline and at 10$^o$ unacceptable. The focus at 80$^o$ is also borderline, but outside the tropics this elevation is only reached around noon near the summer solstice (if at all). Results at low elevations can be improved at the design stage by (a) increasing the tilt angle of the collector axis, currently 30$^o$ (Figure 2a), (b) decreasing the sun elevation at which the mirror corners are aimed perfectly (currently 45$^o$), and/or (c) by deleting the offending mirror units (mainly at the very bottom of the collector aperture); also those units could be turned off-sun during daily startup and shutdown. Note that the first two options degrade the results at high sun elevations. Another option is to reduce the size of mirror units (all of them, or just the problem cases) relative to the collector, with a corresponding increase in their number, and their shape can be changed too (currently a 3:2 rectangle). The effects of three different size/shape options are shown in Figure 6 with sun elevation 10$^o$ — compare to the 10$^o$ image in Figure 5. The same 32 units (indicated in Figure 2(b) from the original 80 units) were used in the calculations, with their axis mounting angles and centre positions unchanged.

Making each mirror unit square by reducing its width increases the total number of units to 120 and is of considerable benefit to collector focus (Figure 6a), but there is still noticeable spill. Reducing the size of the square by 20% each way gives a borderline acceptable result (Figure 6b) and requires 188 units for the same total area. The original rectangle was halved both ways to obtain the largely acceptable focus map in Figure 6(c); 320 units are required. Different sized units could be used in different areas of the collector (smaller units where aims

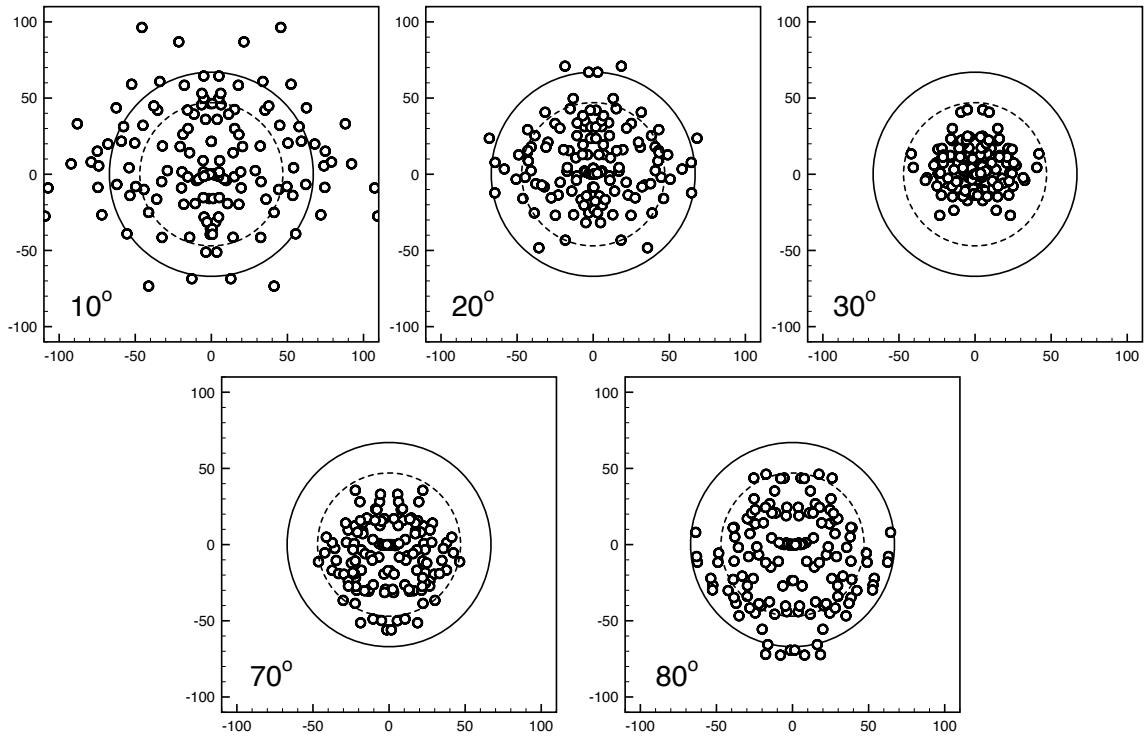


**Figure 5. Focus maps for 750 x 500 mm mirror units at the indicated sun elevations.**

are more degraded) if larger mirror units are a lot cheaper per m$^2$. However, if the ideal size of the PWF 'segmented dish' is an order of magnitude larger than for a conventional dish (see discussion in Bisset, 2016), e.g. 5000 m$^2$, then each of the 320 units for Figure 6(c) would have an area of 16 m$^2$, which is well within the range of sizes for current heliostat designs (Coventry & Pye, 2014) and likely to be quite economical to produce. At 5000 m$^2$ aperture area the aperture radius and maximum rim height would both be about 40 m, and average thermal output would be about 4 MW (see Section 6 following). The conclusion of this analysis is that the original idea of segmenting a paraboloidal surface into 80-100 mirror units is not quite suitable for using a high-performance cavity receiver (CR of order 2000), but 200-320 units will be sufficient.

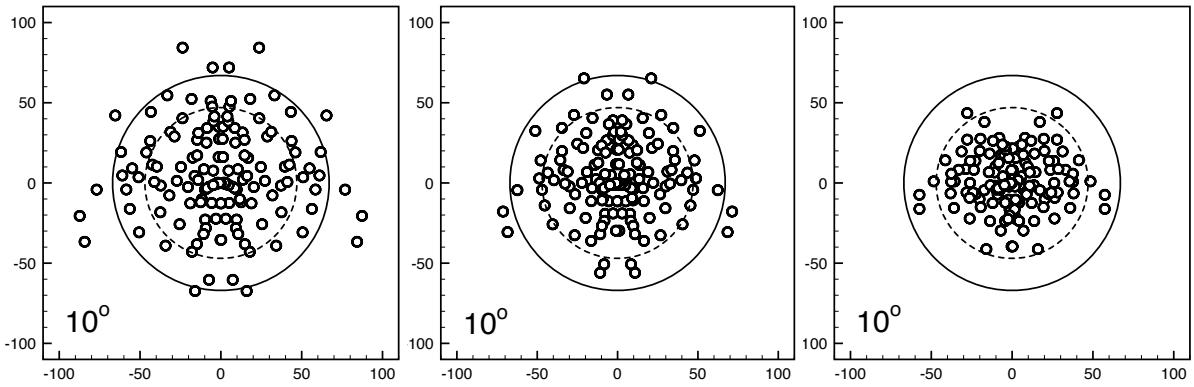


**Figure 6. Focus maps for unit size (a) 500 x 500, (b) 400 x 400, (c) 375 x 250 mm.**

## 5. Heat transport from PWF collectors to thermal storage

New CST power stations usually incorporate some form of thermal storage so that heat supply to the power block is buffered during partly cloudy conditions and electrical output can be time-shifted to match demand. At present the preferred method is sensible heat storage in molten salt, although research on a wide range of methods for collecting, transporting and storing heat is ongoing, as discussed by Ho (2017) and many others. The most likely potential application for PWF collectors is the supply of heat to a molten salt storage system that drives a conventional steam turbine power block, and the latter is likely to have an electrical power in the range 20-100 $MW_e$ or more, since both turbine efficiency and cost per $MW_e$ tend to improve with increasing power. Around 10 to 100 PWF collectors will be needed.

The usual practice for central receiver power plants is to heat the molten salt directly in the receiver, taking care that the salt doesn't freeze when off-sun ( ~200$^o$ C) or decompose when on-sun (~600$^o$ C). If used in multiple PWF collectors, the volume flow rate per collector (and therefore pumping cost) for the salt is quite small, e.g. about 6 or 7 litres/sec for a 5 $MW_{th}$ collector. However all pipework has to be heat-traced, and flexible or rotating joints are required. The entrance to the cavity receiver can be closed off at night so that it stays hot, which greatly simplifies daily startup procedures (see Pacheco, 2002 for the nightmare description of starting Solar Two on a windy day) and the absorber area can be increased because heat loss is far less than for an external-type receiver. Compared to a cavity receiver on a paraboloidal dish, the PWF receiver is an order of magnitude larger and remains at a fixed angle of tilt during operation. Another advantage is that the power to the receiver can be varied over a wide range by bringing groups of mirror units on-sun or off-sun as required, e.g. for startup. In practice, a detailed engineering study would be required before choosing solar salt as the heat transfer fluid, given the likely disastrous effect of salt freezing in the receiver. The alternative is to use a fluid other than salt in the receiver, e.g. molten sodium or a compressed gas, for heat transfer to a heat exchanger adjacent to the molten salt storage.

Molten metals such as sodium have excellent heat transfer characteristics, but also have serious safety concerns and operational problems — see Coventry et al (2015) for a review that includes solar application experience. Molten metals will not be considered further here. The most predictable option for heat transfer is compressed gas, for example air or carbon dioxide at a pressure around 100 bar. Air has no cost or safety concerns, and its behaviour is well characterised, but its heat transfer and transport properties are far from ideal. The combination of high volume flow rates with high temperatures and pressures requires a potentially expensive piping, pumping and heat-exchange system. The heat transfer and pumping properties of $CO_2$ are similar to those of air, but the required volume flow rate is about 2/3 that for air, a substantial saving. The temperature and pressure suggested here are well within the ranges being studied for supercritical $CO_2$ closed Brayton cycle turbines for CST applications (e.g. Stein and Buck, 2017), so the necessary materials properties are understood. Note that although there will be a temperature drop across the gas-to-salt heat exchanger (the gas must leave the receiver at a higher temperature than would the salt), there is no heat loss as such at the heat exchanger, and no effect on overall system efficiency unless temperatures in the cavity receiver increase significantly.

## 6. System efficiency and cost comparisons

It was straightforward to show that a CST power plant based on PWF collectors will be significantly cheaper than a plant based on paraboloidal dishes (Bisset, 2016), but the comparison with central receiver systems was not clear-cut. It is still difficult to give relative costings per $m^2$ of mirror for the two systems, but an estimate of the relative areas of mirror required can be made based on efficiency cascades. The efficiency of heat capture in the molten salt from the energy in sunlight is the product of efficiencies at various stages (interception, reflection, receiver absorption etc) less losses (dispersion, spillage, absorber reflection etc). Factors where there is a difference between a PWF system and a large central receiver system with surround-field of heliostats are given in Table 1. There should be little difference in mirror reflectivity, and spillage is assumed similar although it is very dependent on specific design.

**Table 1. Values used in the efficiency cascade**

| | Central receiver | PWF | Notes |
|---|---|---|---|
| Cosine factor | 0.75 | 0.95 | Based on the paraboloid surface for PWF |
| Shading & blocking | 1.0 | 0.9 | Very low s & b for a well-spaced heliostat field. For PWF, average cosine factor of the collector aperture. |
| Dispersion | 0.97 | 1.0 | Atmospheric dispersion between heliostats and receiver (depends on local conditions and heliostat field size) |
| Absorption at receiver | 0.94 | 1.0 | 5-7% reflection from absorber surface, but mostly trapped in a cavity receiver |
| Receiver efficiency | 0.85 | 0.96 | Averaged over the day (central receiver peak value ~0.89); accounts for radiation and convection losses. |

The cascade products are 0.58 and 0.82 for the central receiver and PWF systems, which means that the PWF power plant requires only 71% of the mirror area of a large central receiver plant. Alternatively it means that the cost of a PWF collector and heat transport system (per $m^2$ of mirror) can be 41% higher than the combined cost of heliostats and receiver (per $m^2$ of heliostat mirror), for equal total cost of system, which allows a lot of room to move. In some respects the PWF collector is actually cheaper because of its single-axis mirror unit mounting, and the modularity of a PWF-based system may be a further advantage in both construction and operation. Detailed designs and costings are needed.

## 7. Conclusion

Results from experiments on a scale model of one mirror unit from a PWF collector were sufficiently in agreement with numerical model results to give confidence in the numerical methods. When applied to the whole aperture of a collector at a wide range of sun elevations and using a concentration ratio of 2000 at the target, the numerical model indicated that spillage of reflected rays from the corners of some mirror units was excessive. The solution is to increase the number of mirror units per PWF collector from 80 up to 180-320. Compared to

a central receiver CST plant with a surround-field of heliostats, the PWF collector with cavity receiver has a significantly better average cosine factor and significantly better receiver efficiency. It also avoids both atmospheric dispersion and reflection from the absorber surface. As a result, the area of mirror (and the corresponding equipment for supporting and aiming mirrors) required for a PWF system is about 70% of that of a central receiver system. The comparative cost per $m^2$ of mirror is not known, but should be similar given the simple single-axis rotation of mirror units on their base-frame. Modularity in design, construction and operation is a further advantage.

## References

Baum, V, Aparasi, R, Garf, B, 1957, 'High-power solar installations', *Solar Energy* **1** (1) p6-12

Bisset, D, 2016, 'Testing the 'Segmented Dish' Piecewise-Focusing Solar Collector', in *Proc Asia Pacific Solar Research Conference 2016*, Australian PV Institute, ISBN: 978-0-6480414-0-5 http://apvi.org.au/solar-research-conference/wp-content/uploads/2017/05/D-Bisset-Testing-the-%E2%80%98Segmented-Dish%E2%80%99-Piecewise-Focusing-Solar-Collector.pdf

Coventry, J, Andraka, C, Pye, J, Blanco, M, Fisher, J, 2015 'A review of sodium receiver technologies for central receiver solar power plants', *Solar Energy* **122** p749-762

Coventry, J, Andraka, C, 2017, 'Dish systems for CSP', *Solar Energy* **152** p140–170

Coventry, J, Pye, J, 2014, 'Heliostat cost reduction — where to now?' Presented at SolarPACES 2013. *Energy Procedia* **49** p60–70

Ho, C K, 2017, 'Advances in central receivers for concentrating solar applications', *Solar Energy* **152** p38–56

Jones, D, 1982, 'Heliostatic solar energy conversion system'. Patent US4365618

Kim, J, Kim, J-S, Stein, W, 2015, 'Simplified heat loss model for central tower solar receiver', *Solar Energy* **116** p314–322

Kolb, G, Jones, S, Donnelly, M, Gorman, D, Thomas, R, Davenport, R, Lumia, R, 2007, *Heliostat Cost Reduction Study*, Sandia National Laboratories, SAND2007-3293

Lovegrove, K, Burgess, G, Pye, J, 2011, 'A new 500 $m^2$ paraboloidal dish solar concentrator', *Solar Energy* **85** p620–626

Pacheco, J (ed), 2002, *Final Test and Evaluation Results from the Solar Two Project,* Sandia National Labs, SAND2002-0120

Pye, J, Hughes, G, Abbasi Shavazi, E et al, 2015, 'Development of a Higher-Efficiency Tubular Cavity Receiver for Direct Steam Generation on a Dish Concentrator', SOLARPACES 2015, AIP Publishing LLC, South Africa, p030029

Ruiz, V, Frasquet, M, Martínez, F, Silva, M, Lillo, I, Díaz Andrades, F, Lobo Márquez, G, 2014, 'The variable geometry central receiver system concept. First results and comparison with conventional central receiver systems', *Energy Procedia,* **57,** p2255– 2264

Sánchez-González, A, Rodríguez-Sánchez, M, Santana, D, 2016, 'Aiming strategy model based on allowable flux densities for molten salt central receivers', *Solar Energy*, http://dx.doi.org/10.1016/j.solener.2015.12.055

Stein, W, Buck, R, 2017, 'Advanced power cycles for concentrated solar power', *Solar Energy* **152** p91-105